CAA Proposal:
Search for a $S = +1$ $Z^+(1530)$ Resonance at CLAS

Spokesperson: Ken Hicks (Ohio U.)
Participants: Will Brooks (JLab), Daniel Carman (OU),
Eugene Pasyuk (ASU), Reinhard Schumacher (CMU),
Elton Smith (JLab), Stepan Stepanyan (JLab/ODU),
Dave Tedeschi (SC), Luminita Todor (CMU)

October 24, 2002

1 Introduction

The Z^+ was proposed by Diakonov, Petrov and Polyakov [1] in the chiral soliton model theoretical framework. Their model predicts an anti-decuplet in anology to the usual decuplet of SU(3), except that the anti-decuplet has objects with exotic quantum numbers, such as the $S = +1$ resonance with a $(uudd\bar{s})$ quark structure, called the Z^+. The Z^+ can also be thought of as a kaon-nucleon (K^+n or K^0p) bound state, and does not violate any rules of QCD. Using mass splitting parameters similar to the Gell-Mann-Okubo relation, the mass of the Z^+ is predicted at 1.53 GeV with a narrow width of 15 MeV.

Whether the theory for the Z^+ is correct or not is unimportant here. The LEPS collaboration at the SPring-8 facility [2] has found a sharp peak in the missing mass spectrum of K^- photoproduction from the reaction $\gamma + n \rightarrow K^- + Z^+$ where the Z^+ decays to a $K^+ + n$. This peak is seen at a mass of 1.54 GeV with a width of 10 MeV or less. Independent analysis by different members of the LEPS collaboration, using different cuts, all find evidence of this peak, which has a statistical significance of 5-6 σ depending on the background shape, which is reasonably described by data from a LH_2 target (with no neutron sources). The results will be submitted to PRL by the end of November, and will be available on the usual preprint servers (lead author T. Nakano).

It is important to search for the Z^+ at other facilities in order to confirm or deny the result. Searches using kaon beams [3] are not ideal due to the low beam momentum necessary to form this narrow resonance. The CLAS spectrometer has already taken data on a LD_2 target, and preliminary simulations indicate about a 1% acceptance for detection of the Z^+ (using the predicted mass and a phase-space production cross section).

To date, several preliminary analyses have been performed using the g2 data set.One method, given in section 2, is to follow the path used by the SPring-8 analysis, where a coincident K^+ and K^- are detected, and the missing mass of the K^- is calculated with cuts to exclude the $\phi(1020)$ and the $\Lambda(1520)$ backgrounds. Another method, given in section 3 and already used by Stepan Stepanyan in a preliminary study, is to look for the p and π^- from decay of the Λ ground state in coincidence with either a $K^+(n)$ or $p(K^0)$ from decay of the Z^+. Yet another method would be to look for the K^- and p that have the missing mass of a K^0, and search for a peak in the K^- missing mass.

2 Inclusive Analysis: the K^+K^- final state

The analysis groups will initially focus on the g2 data for coincident K^+K^- events, following the approach of the SPring-8 analysis. Preliminary analysis of these data is described below. It should be noted, however, that this analysis has not been subjected to the same stringent systematic checks that are done for analysis notes. The results presented here could change upon further investigation.

The K^+ and K^- particles are very loosely defined in the g2 data. Although there are about 2 million events with a nominal K^+ and K^- identified by the data cooking, most of these events are background, as shown in Fig. 1, where the mass of the K^+ and K^- have been calculated from the momentum and beta of particles having an ID for the kaon. The top two plots show the mass with no cuts, and only a hint of a peak at the kaon mass of 0.494 GeV. The lower two plots have an additional requirement on the mass of the opposite sign kaon, which enhances the signal to noise.

Much of the background is due to misidentified pions. This is clearly seen in Fig. 2 where bands in momentum are seen to cross over the mass spectrum in the top plots (due to choosing the wrong RF bucket in the cooking) which have the same cuts as the previous figure (cut on opposite charge kaon mass). These plots can be cleaned up considerably as shown in the lower plots of Fig. 2 where additional cuts have placed on the the calculated missing mass (shown below) and other standard cuts (vertex, number of photons in the tagger, number of detected particles, a range of photon energy between 1.6-2.3 GeV, and kaon momentum below 1.1 GeV/c). The cleaned-up mass spectra show that kinematic constraints can significantly reduce the background from misidentified particles.

The missing mass and invariant mass are easily calculated for the events that pass the standard cuts given above, and are shown in the top plots of Fig. 3. The peak corresponding to the nucleon mass (spread by Fermi momentum and uncertainties in the photon energy) is seen at 0.93 GeV in mm_{KK}. In the invariant mass spectum, m_{inv}, a sharp peak is seen due to the $\phi(1020)$. The broad structure near 1.22 is of unknown origin, but may be due to the detector acceptance. The bottom plots have been cut additionally by a range of mm_{KK} corresponding to the expected range of the nucleon mass.

The missing mass for the K^+ and K^- can be calculated from knowledge of the photon energy and the 4-momentum of the kaon. These spectra are shown in Fig. 4

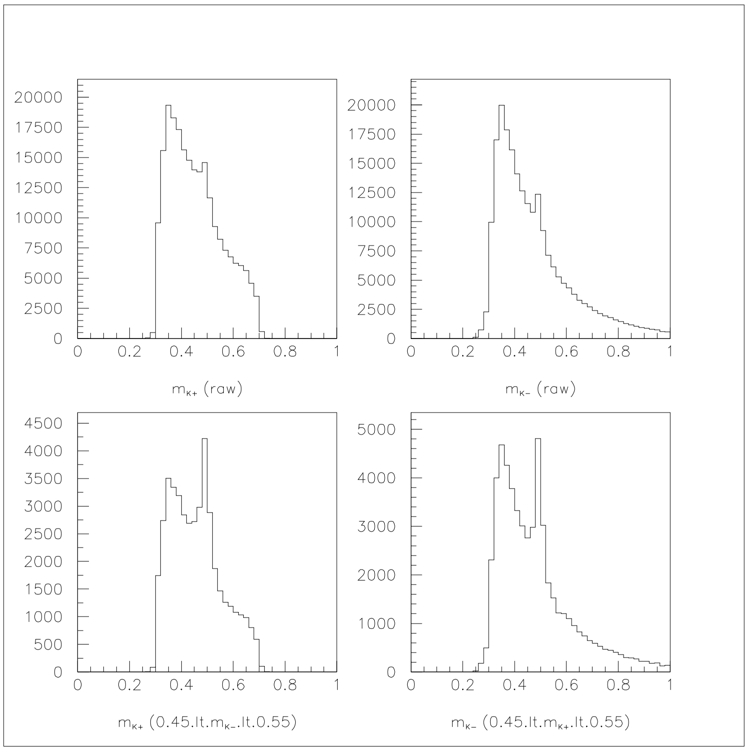

Figure 1: Mass of the K^+ and K^- without cuts (top) and with cuts shown (bottom).

for the same cuts as in the previous figures (missing mass and standard cuts). No peak is seen for either the $\Lambda(1520)$, which is expected to be present in the K^+ missing mass, or the $Z^+(1530)$ in the K^- missing mass spectrum.

Also shown in Fig. 4 are 2-dimensional plots of mm_K versus the total missing mass of both kaons mm_{KK}, which is cut on the expected mass of the nucleon. The 2-D figures show a clear diagonal trend to the data, with sharp boundaries that can be shown to be due to the photon energy range cut. Following the SPring-8 analysis, we will correct the kaon missing mass for the "missing energy" due in part to the uncertainty in the measured photon energy. The correction may be explained as follows: the photon energy is common to both the kaon missing mass calculation and the total (KK) missing mass. By using the resolution of the CLAS spectrometer, we can correct for the uncertainty in "missing energy" (either the photon energy or the z component of the Fermi motion).

After correction for the missing energy, the missing mass for the K^+ (top) and K^- (bottom) are shown. The same correction and cuts have been applied to both K^+ and K^- spectra. A clear peak is seen at the mass of the $\Lambda(1520)$ in the top plot and a narrow peak has now appeared near the expected location of the Z^+ in the bottom plot. The width of the Z^+ peak is surprisingly narrow, and at the present time we can not say if this is due to an instrumental problem or if it is real physics. However, it is curious that a similarly narrow peak was seen in the SPring-8 data at nearly the same mass (for the same reaction), and the chance that both observations are instrumental errors seems unlikely. Note that the position and width of the peak depends on the

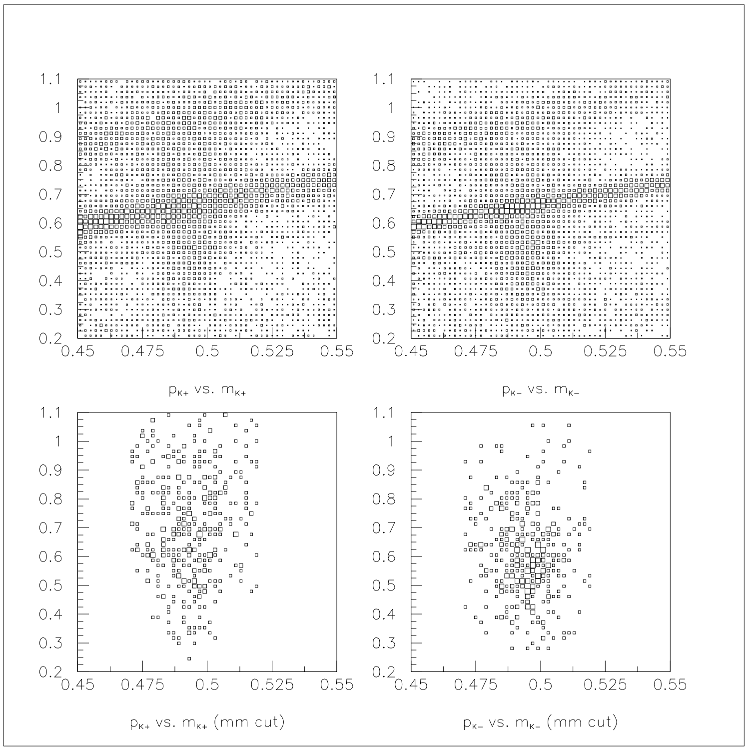

Figure 2: Momentum versus mass of the K^+ and K^- with mimimal cuts (top) and with additional kinematic cuts (bottom).

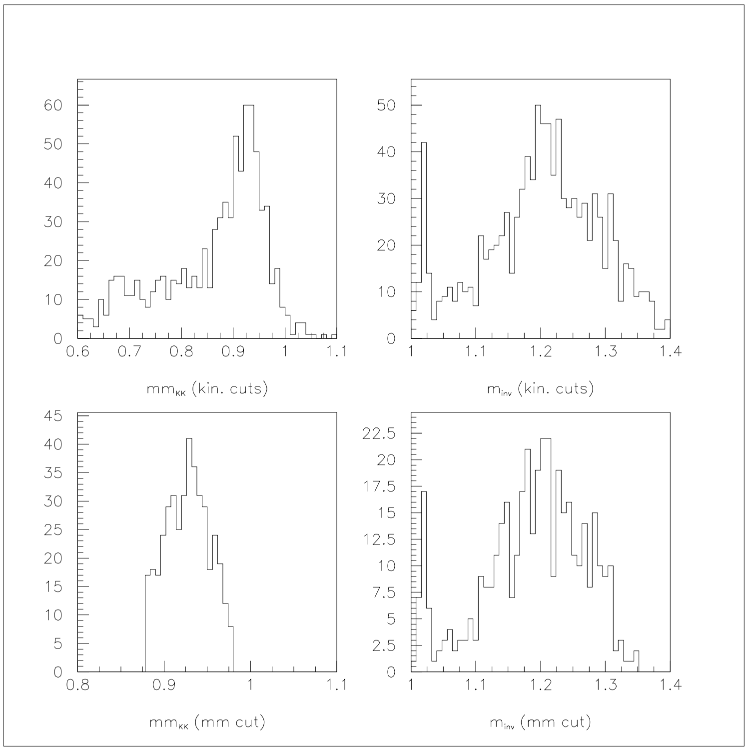

Figure 3: Missing mass and invariant mass of the KK system for standard cuts (top) and the additional mm_{KK} cut shown (bottom).

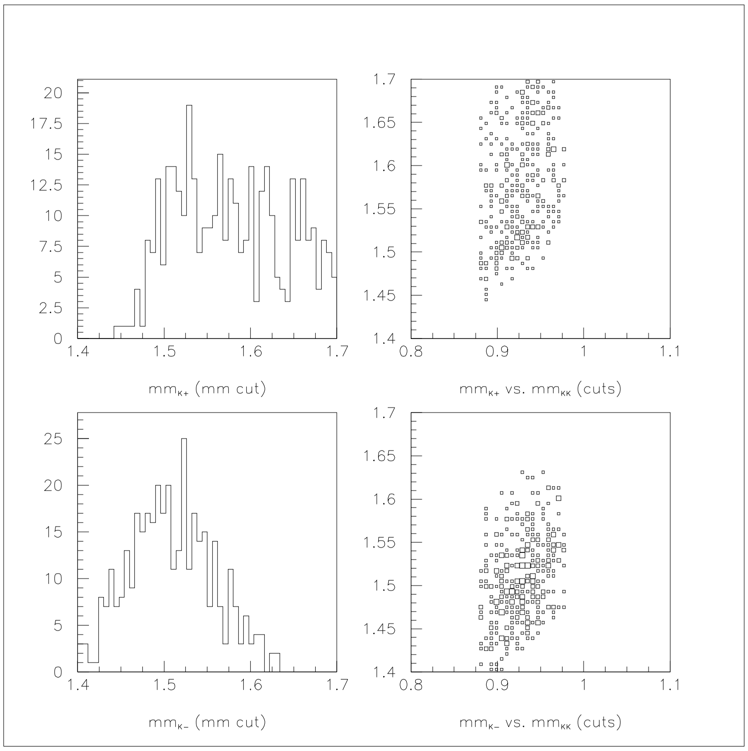

Figure 4: Missing mass of the K^+ and K^- (left) and 2-D plots of the kaon missing mass versus the full missing mass.

detector calibrations, and could change upon refinement of the particle momenta.

The photon energy dependence of the missing masses are shown in Fig. 6 in order to demonstrate that the peak is not limited to a single photon energy (due to a bad E or T counter). Also shown is a 2-D plot of the correlations between the missing masses. The vertical lines correspond to the region of the $\Lambda(1520)$, which are spread across the range of the K^- missing mass (as expected from kinematic of its decay). To show that the Z^+ peak is not an artifact of the $\Lambda(1520)$, the missing mass of the K^- has been plotted with a cut (shown on the 2-D plot) to eliminate events in this range of the K^+ missing mass. The "background" in the K^- missing mass spectum has been reduced, but the peak is still quite clear.

We propose to continue examining the g2 data to understand if the peak seen in the K^- missing mass is real, and whether it can be associated with the predicted Z^+ resonance. If so, then this would be an exciting confirmation of the SPring-8 results and could lead to new theoretical calculations of meson-baryon molecular states.

3 Exclusive Reactions in γD Interactions

Direct production of the Z^+ resonance using kaon beams is difficult since it requires low beam energy. While it is problematic to bring low energy kaons to the target, one can try to bring the "target" to the kaon. In other words, by the process of embedding kaon production inside the nuclei, one can seek a reaction channel when

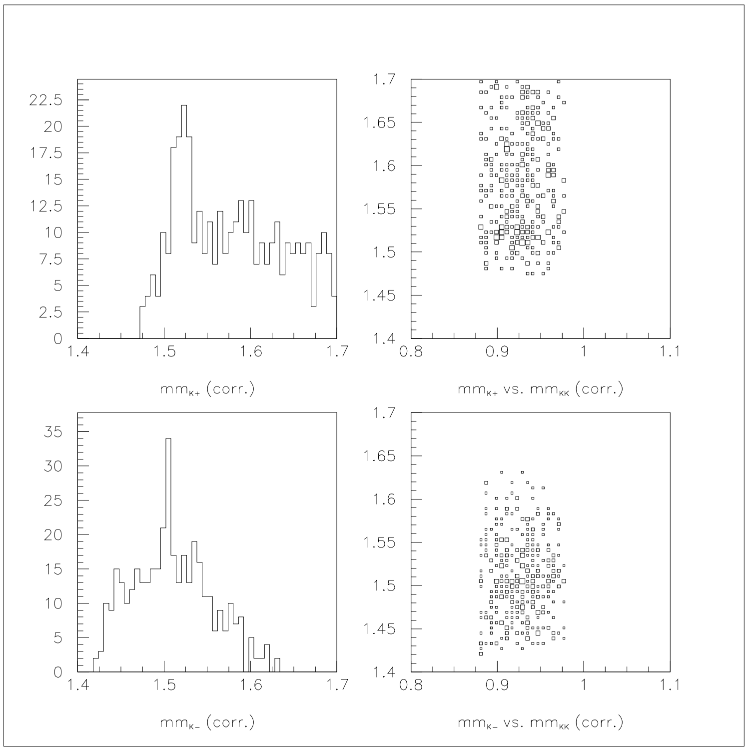

Figure 5: Missing mass of the K^+ and K^- corrected for "missing energy" shown by the 2-D plots.

a low energy kaon, produced on one of the nucleons in nucleus, interacts with other nucleon forming the possible S-channel resonance.

Photoproduction on deuterium is a clean way of doing this type of measurement. Photoproduction of a kaon can proceed either via production of a hyperon or production of a $\phi(K^+K^-)$ on a nucleon. By selecting a particular final state one can effectively select a specific process when produced kaon scatters on other nucleon.

In this analysis three topologies of final state are studied:

- $\gamma D \to \pi^- p K^+ X$, with $\pi^- p = \Lambda$ and $X = n$ (Fig. 7);
- $\gamma D \to \pi^- p p X$, with $\pi^- p = \Lambda$ and $X = K^0$ (Fig. 7);
- $\gamma D \to p K^+ K^- X$, with $X = n$ (Fig. 8);

One more final state is possible in the reaction presented in Fig. 8, $\gamma D \to ppK^-(K^0)$. However this final state was not studied yet.

3.1 Data sets and event skim

We use g2a data taken during the August-September of 1999, using two electron beam energies 2.478 and 3.115 GeV. For preliminary analysis ntuples (#10) produced during the "Pass1/v2" cooking have been used. The whole data set for both energies was skimed twice, first to select events with π^- and two positive particles, and second to

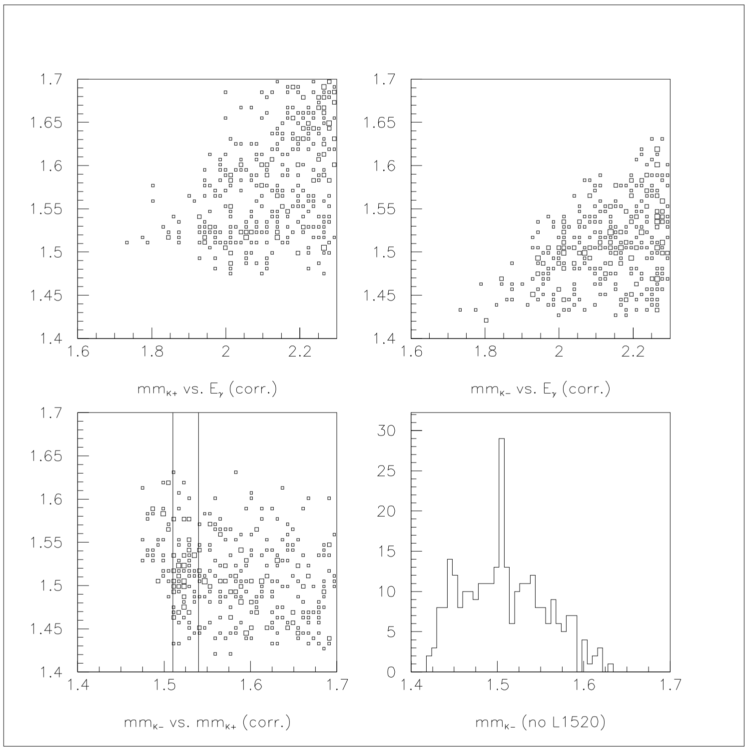

Figure 6: Missing mass of the K^+ and K^- plotted versus the photon energy and also versus each other. The 1-D spectrum has an additional cut to remove the $\Lambda(1520)$ contribution, shown by the lines in the 2-D plot.

select a proton and K^+K^-. In addition, during the skim ntuple#10 was reduced to a ntuple with fewer parameters in order to put the whole data set in one file. The skim used very lose cuts for PID selection. After cuts on the invariant mass and missing mass distributions of final state particles, particle identification ambiguities were resolved due to the overconstrained kinematics.

3.2 Reaction $\gamma D \to \Lambda^0 Z^+$

This reaction is selected by identification of the Λ^0 via its decay to $\pi^- p$, and the Z^+ from K^+n or K^0p decay. In all final state topologies we have a proton and a π^- detected from the lambda decay, and the K^+ or the second proton detected from the Z^+ decay. Missing particles, n or K^0, are identified via missing mass.

3.2.1 Final state $\gamma D \to \Lambda K^+(n)$

In Fig. 9 the mass of the missing system in the reaction $\gamma D \to \pi^- p K^+ X$ is plotted against the invariant mass of the $\pi^- p$. One can clearly see high concentration of events around the $\pi^- p$ invariant mass 1.115 GeV, corresponding to the ground state lambdas, correlated with missing mass around 0.94 GeV, corresponding to the missing neutron. Having a $\pm 2\sigma$ cut around Λ^0 mass, and a $\pm 3\sigma$ cut around neutron mass, we selected the reaction $\gamma D \ \to \ \Lambda^0 K^+(n)$.

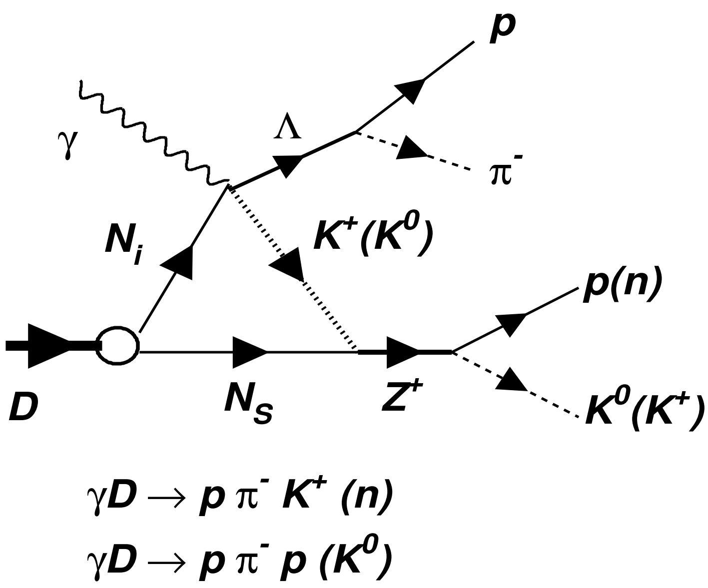

Figure 7: Diagram corresponding to the production of the Z^+ in the two step processes via production of the ground state lambda in the γD interactions.

The distribution in Fig. 9 corresponds to the event sample from the 2.478 GeV running. Similar distribution has been obtained for the 3.115 GeV data set as well.

The Z^+ should appear as a resonance in the K^+n system or, equivalently, as a resonance in the missing system of reaction $\gamma D \to \Lambda X$. One should note that in the determination of the M_{Z^+} only four-momenta of the final state proton and the π^- enter, and there are *no uncertainties due to Fermi motion.*

$$M_{Z^+}^2 \;=\; P_{Z^+}^2 \;=\; (P_n + P_{K^+})^2 \;\equiv\; (P_\gamma + P_D - P_p - P_{\pi^-})^2 \tag{1}$$

After the selection of the reaction, two more cuts have been applied to the data. The first cut is on the momentum of the missing neutron. To cut out events when the neutron was a spectator (when quasi-free production of the ground state lambda took place on the proton and the kaon escaped the nucleus without interacting with the neutron), we require neutron momentum to be larger than 0.3 GeV/c, above the Fermi momentum range.

The second cut is on the kaon momentum. A simple simulation of the kinematics of the reaction $\gamma D \to \Lambda^0 Z^+$, where $M_{Z^+} = 1.53$ GeV and $\Gamma_{Z^+} = 10$ MeV, shows that the kaon momentum distribution peaks around 0.4 GeV/c and almost no kaons with $p_K > 1$ GeV, while in the data there are many high momentum K^+s. A cut $p_K < 1$ GeV was applied to match the momentum distributions from data and from the simulation.

In Fig. 10 final distributions of K^+n invariant mass is shown for both beam energies and for a $\pm 2\sigma$ and a $\pm 3\sigma$ cut on the missing neutron mass. In all cases a $\pm 2\sigma$ is made on the invariant mass of the $\pi^- p$ to select lambdas. Background in the distributions of Fig. 10 are estimated using events in the $3\sigma(2\sigma)$ bands on the tail of the missing neutron mass distributions at a distance of $\pm 5\sigma$ from the peak. Final nK^+

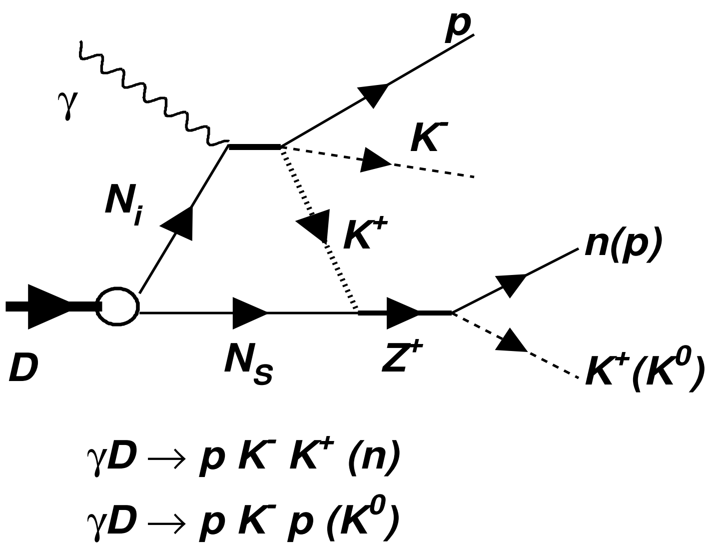

Figure 8: Diagram corresponding to the production of the Z^+ in the two step processes by production of K^-K^+ pair in the γD interactions.

invariant mass distributions, after background subtraction with both beam energies combined, is presented in Fig. 11. The statistics is poor, but a structure around the predicted Z^+ mass is visible. In Fig. 11 the first elevated point is on the mass 1.54 GeV.

3.2.2 Final state $\gamma D \to \Lambda p(K^0)$

In the case when Z^+ decays to pK^0 we detect two protons and the π^-. In Fig. 12 distribution of the missing mass squared of K^0 versus invariant mass of the π^-p is shown. Combinations with both protons are included. Spot corresponding to the Λ^0 and K^0 is clearly visible. $\pm 2\sigma$ cuts on the invariant mass of the π^-p and on the missing mass of the $pp\pi^-$ were used to select reaction $\gamma D \to \Lambda p(K^0)$.

For the final selection a cut on the kaon momentum, $p_K < 1$ GeV/c, is used as in the previous case. In Fig. 13 distribution of pK^0 invariant mass is shown before and after momentum cut. One should note that this selection has much larger background in the missing kaon identification, than it was in the case of a missing neutron.

Background was subtracted in the same way as for K^+n channel. Events from side bands of kaon missing mass squared distributions have been used. For background subtraction mass distributions were rebinned to have 20MeV per bin. In Fig. 14 background subtracted distributions of pK^0 invariant mass for both energies and for both proton combinations are shown. The distribution for only the first proton summed for both energies is shown in Fig. 15.

After background subtraction the distributions for the two decay channels have been combined. In Fig. 16 final distribution of the missing mass in the reaction $D(\gamma, \Lambda^0)X$ is shown for events from both decay channels, and from both beam ener-

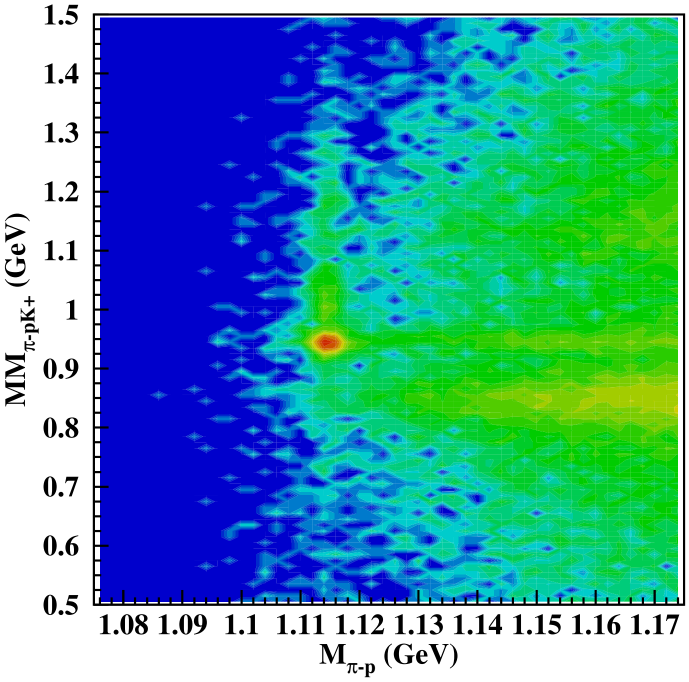

Figure 9: Missing mass vs invariant mass $\pi^- p$ in the reaction $\gamma D \to \pi^- p K^+$ for the 2.478 GeV data set.

gies. The elevated point is at 1.54 GeV, however the statistics is too small to draw conclusions.

3.3 Final state $\gamma D \to p K^+ K^- (n)$

The reaction in Fig. 8 can proceed via production of a ϕ meson (on-shell or off-shell) on the proton, then scattering of a K^+ from ϕ decay on the neutron. Alternatively it may proceed via production of an exited state hyperon, like the $\Lambda(1520)$, and then scattering of K^+ on the neutron. Final events were selected first using broad cuts on the K^+ and K^- masses, then by comparing vertex time for kaons against proton vertex time. Events that have time difference on the vertex for both kaons less than ± 1 ns relative to the proton were selected for final analysis.

In Fig. 17 the missing mass squared and missing momentum distributions in the reaction $D(\gamma, p K^+ K^-) X$ are presented. Distribution has a peak around the neutron mass with almost no background. This indicates clean identification of kaons, and therefore reaction $\gamma D \to p K^+ K^- (n)$.

For further analysis a $\pm 3\sigma$ cut is applied on the missing neutron mass squared. A cut on the invariant mass of the $K^+ K^-$ was also used to cut out ϕ meson when the K^+ did not interact with the neutron.

After cutting on $P_M > 0.2$ GeV, the invariant mass of the $K^+ n$ system is shown in Fig. 18 without (left) and with (right) a cut on the $\Lambda(1520)$ mass (invariant mass

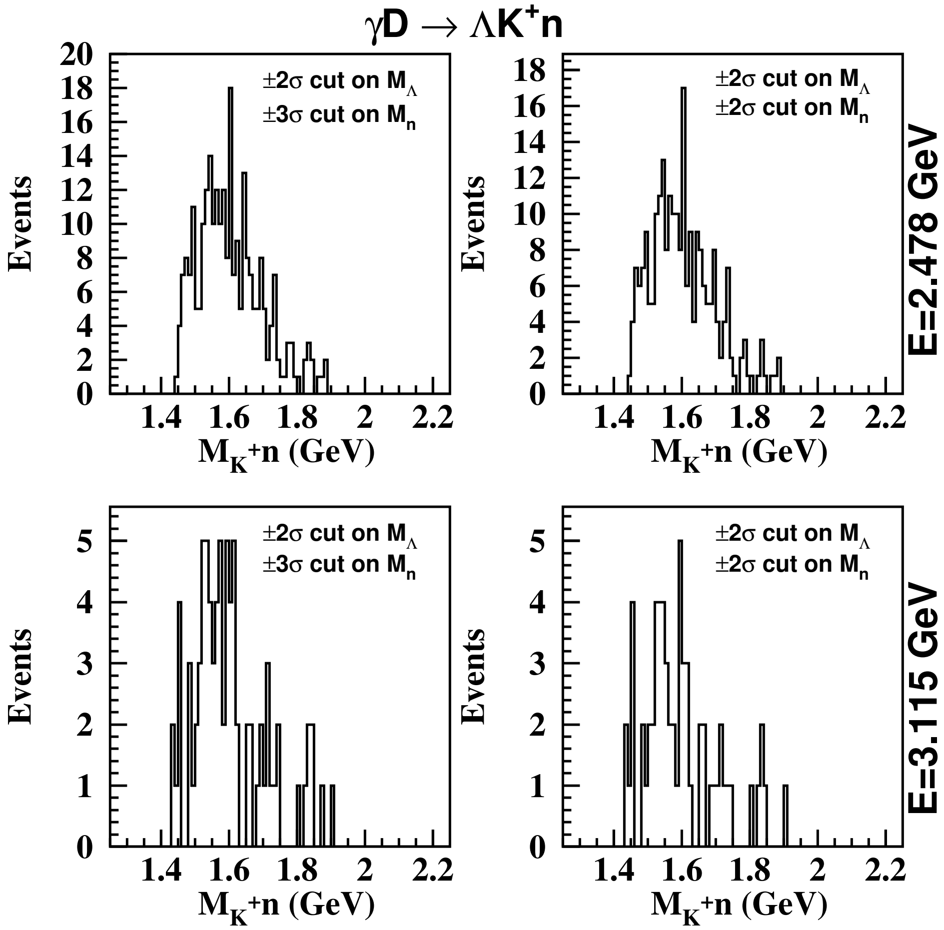

Figure 10: Distribution of events after all cuts. Top row is for data set at 2.478 GeV and the bottom row is the data at 3.115 GeV. For both beam energies $\pm 2\sigma$ cut is applied on $p\pi^-$ invariant mass to select Λs. For plots on the left events are selected within $\pm 3\sigma$ of the mass of a missing neutron, on the right are within $\pm 2\sigma$.

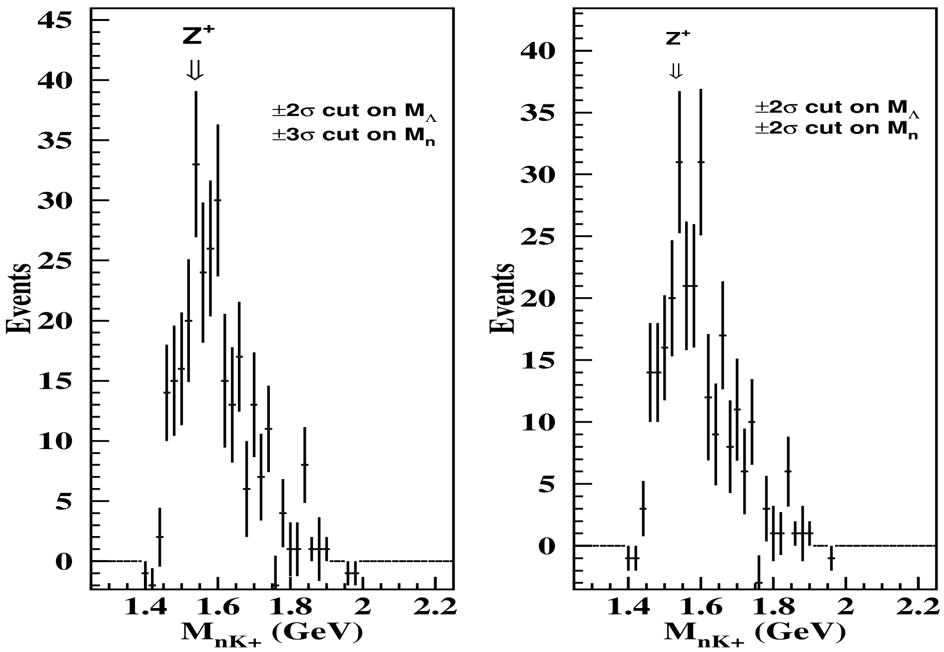

Figure 11: Distribution of the nK^+ invariant mass for whole data set (sum of the two beam energies).

of the pK^-). Again, the statistics is poor but the enhancement around 1.54 and 1.63 GeV are evident.

4 CLAS Analysis Plan

The general goal is to analyze any existing data set to search for the Z^+ peak seen by the SPring-8 LEPS collaboration. The most natural starting point is the g2 data set, which used a liquid deuteriium target with CLAS configured for real photons. This data set has already been calibrated, cooked, and skimmed for kaons. The g2 runs will be the first target of the Z^+ search. Other promising data sets are the e5 and g3 runs. The proposal here is to look for the Z^+ in **any** of the CLAS data taken before October, 2002, although the initial searches will focus on the g2 and e5 data.

Several independent analyses will be done by the participants listed above. It is natural to have one analysis group centered at Ohio, led by Ken Hicks who has detailed knowledge of the SPring-8 analysis, and other analyses done elsewhere. Each analysis group use their own software and background cuts, and investigate methods to deal with Fermi motion. This structure will allow a quick cross check of possible evidence for the Z^+, and will guard against a particular bias in a single analysis procedure.

Each analysis team will decide how to approach the analysis in a way that seems

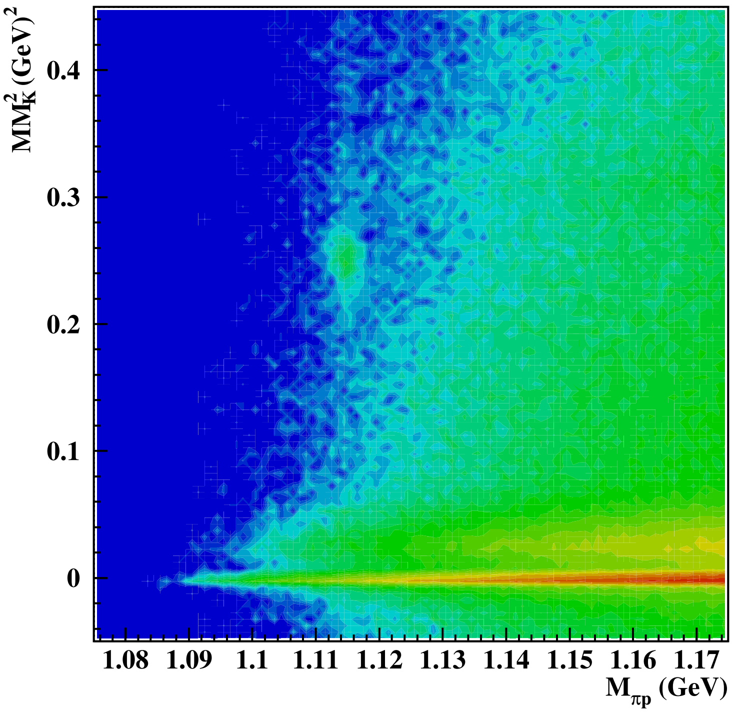

Figure 12: Missing mass squared of K^0 vs invariant mass of the $\pi^- p$. Combinations with both protons are included.

the most promising way to search for the Z^+. In all cases, a key step will be how to elimnate the background from competing reaction channels. It is important to address threshold effects and cuts that could limit phase space in such a way as to create a false peak. Much attention will be devoted to determining background sources and instrumental effects that might confuse the interpretation of any unusual peaks in the data.

References

[1] D. Diakonov, V. Petrov, and M. Polyakov, Z. Phys. A **359**, 305 (1997).

[2] T. Nakano *et al.*, Nucl. Phys. **A670**, 332 (2000); T. Nakano, presentation at PANIC 2002, to be published.

[3] R. Arndt *et al.*, Phys. Rev. D **46**, 961 (1992).

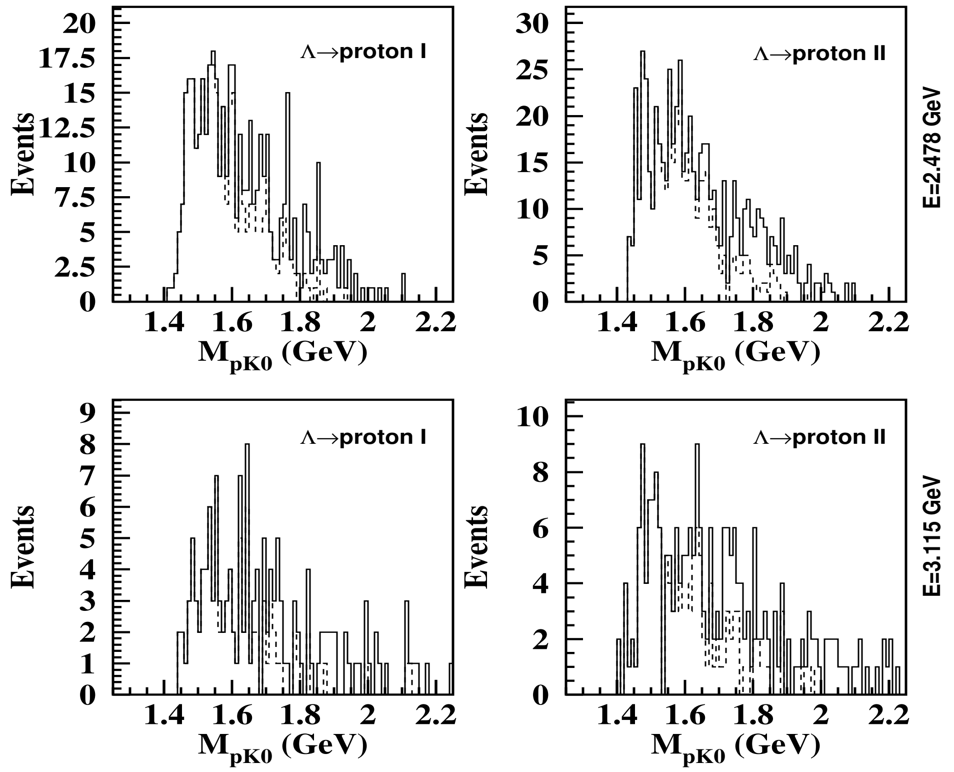

Figure 13: Distribution of the pK^0 invariant mass before, solid line histogram, and after, dashed line histogram, $p_K < 1$ GeV cut.

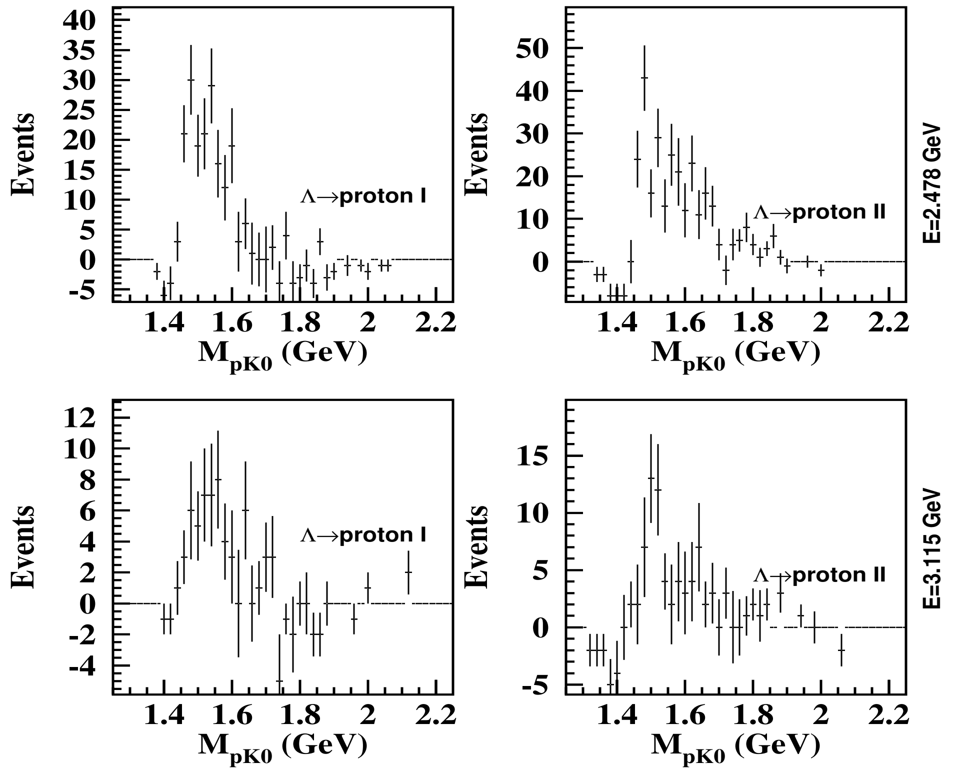

Figure 14: Distribution of the pK^0 invariant mass after background subtraction using side bands on K^0 mass distribution.

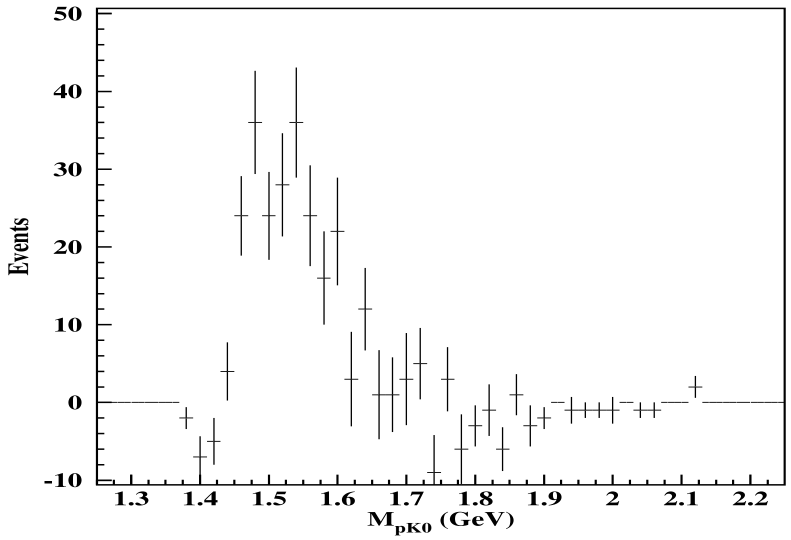

Figure 15: Background subtracted distribution of pK^0 invariant mass summed over events for both data sets, and for the first proton only.

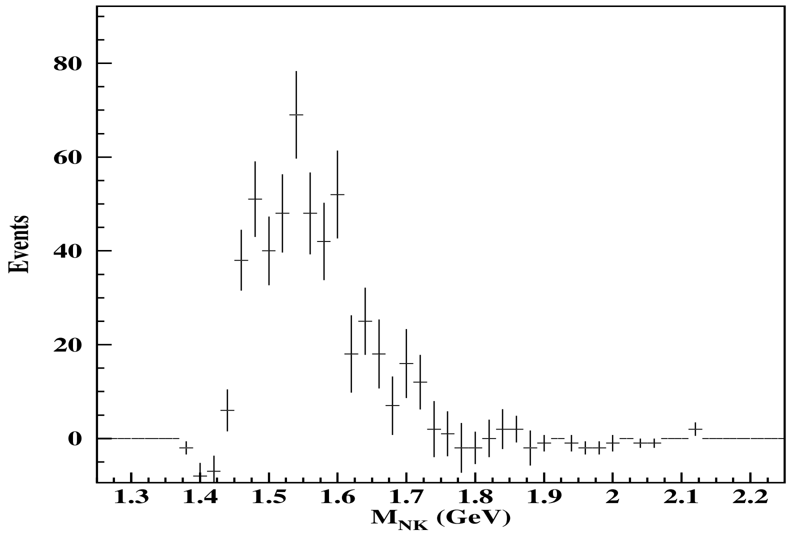

Figure 16: Final distribution of the KN invariant mass for both decay mode of Z^+. Events from two beam energy settings are combined.

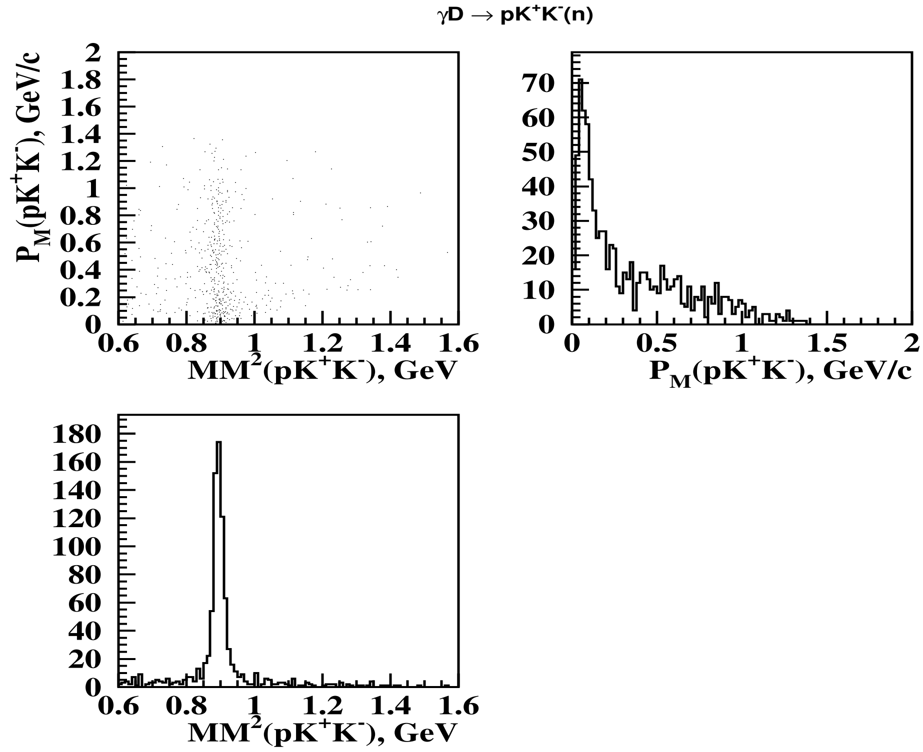

Figure 17: Missing mass squared and missing momentum distributions of $\gamma D \to pK^+K^-X$ reaction after vertex time cuts for kaons.

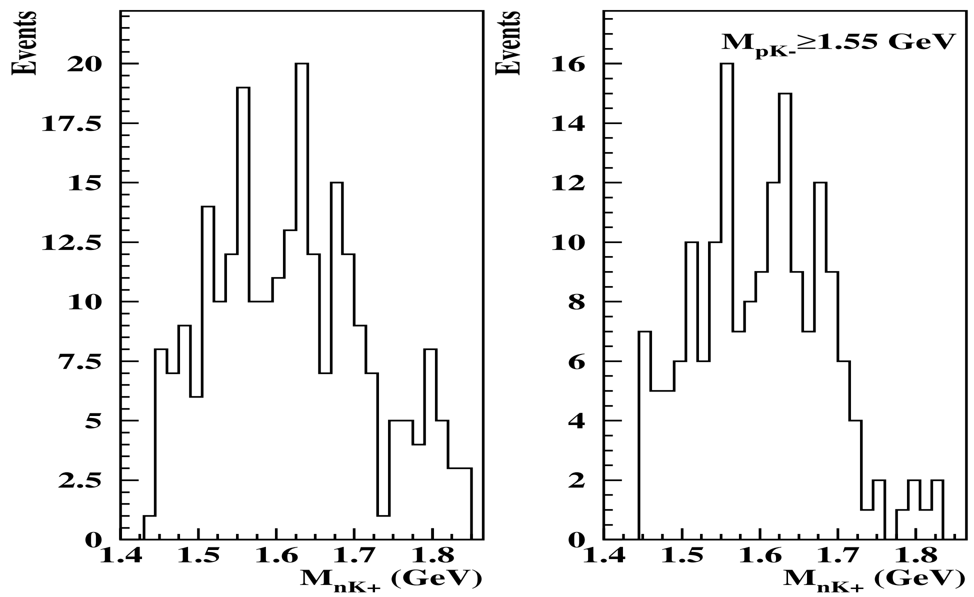

Figure 18: The distribution of the K^+n invariant mass in the reaction $\gamma D \to pK^-K^+(n)$.